

# Frequency-domain spectroscopy

Sergio Fantini<sup>1</sup>, Beniamino Barbieri<sup>2</sup>, Maria Angela Franceschini<sup>1</sup> and Enrico Gratton<sup>1</sup>

<sup>1</sup>Laboratory for Fluorescence Dynamics, Department of Physics, University of Illinois at Urbana-Champaign, 1110 West Green Street, Urbana, Illinois 61801-3080, USA and <sup>2</sup>ISS, Incorporated, 2604 North Mattis, Champaign, Illinois 61821, USA

**ABSTRACT.** Frequency-domain spectroscopy employs a light source whose intensity is modulated at a radio frequency ( $\sim 10^8$  Hz). Such a modulated signal contains a richer information content than the steady-state signal and allows the analysis of time dependent processes such as the fluorescence decay and light transport in turbid media. We describe the instrumentation and the measurement technique we have used in frequency-domain spectroscopy. The basic technique involves down conversion of the radio frequency signal to a lower frequency that is then digitally processed to yield the average value, amplitude, and phase of the original signal. We finally cite applications of the frequency-domain method in the fields of fluorescence spectroscopy and photon migration.

## 1. INTRODUCTION

Steady state measurements, which employ time-independent light intensities, are generally inappropriate to study dynamic processes in spectroscopy, or to determine the optical parameters of random media. For instance, the measurement of the fluorescence decay time and the determination of absorption and scattering coefficients in optically turbid media require the use of time-resolved spectroscopy. Time-resolved spectroscopy can be performed in either the time-domain or in the frequency-domain, depending on the time structure of the light source emission and on the detection system. In this Chapter, we describe frequency-domain spectroscopy, in which the source intensity is either pulsed or sinusoidally modulated. By appropriately isolating harmonic waves, one can define and measure

three independent parameters, namely the average value of the light intensity and the amplitude and phase of each wave. This richer information content with respect to steady state spectroscopy, where the intensity is the only measurable parameter, results in the extended capabilities of frequency-domain spectroscopy.

## 2. BASIC PRINCIPLES OF THE FREQUENCY-DOMAIN TECHNIQUE

The key feature of frequency-domain spectroscopy is the modulation of the intensity of the light source. If the intensity is sinusoidally modulated at a frequency  $f$ , one can define three parameters: the average intensity ( $I_{dc}$  or dc intensity), the amplitude of the intensity oscillations ( $I_{ac}$  or ac amplitude), and the phase of the wave ( $\Phi$ ) with respect to some arbitrary phase. These parameters, which completely describe and characterize the sinusoidally modulated wave, are the quantities of interest in frequency-domain spectroscopy. On the basis of these definitions, the intensity modulated signal can be written as follows:

$$I = I_{dc} + I_{ac} \cos(\Phi - \omega t), \quad (1)$$

where  $\omega$  is the angular modulation frequency ( $\omega = 2\pi f$  with  $f$  modulation frequency). The acronyms dc and ac are derived from electronics terminology where dc means *direct current* and ac means *alternating current*. The similarity in the two approaches is the steady state aspect of the dc intensity (or current) as opposed to the time varying character of the ac signal. In frequency-domain spectroscopy, the ratio between the ac

amplitude and the dc intensity is also widely used. This ratio ( $I_{ac}/I_{dc}$ ) is called modulation ( $m$ ). In some applications, phase and modulation are the only parameters of interest. For this reason, the frequency-domain approach is sometimes designated by the term *phase-modulation* (which should not be confused with phase modulation methods in radio technology, where the phase of a carrier signal is actually modulated). Somewhat less justified and potentially confusing are other terms, such as *frequency modulation* or *amplitude modulation*, which can also be found in the literature to indicate frequency-domain methods. In the frequency-domain there is no carrier signal, so that there is no modulation of one of its parameters (amplitude, frequency, or phase). For this reason, we will use the terms "frequency-domain," and "intensity modulation of the light source."

In a spectroscopy experiment, the light signal is sent to the sample and a portion of the light transmitted or reflected is collected after it has somehow interacted with the sample. From the frequency-domain point of view, the interaction with the sample causes changes in the dc, ac, and phase of the intensity wave. The information provided by the dc signal is the same as that obtained by steady state spectroscopy. However, the ac signal has additional information content since the interaction of the intensity modulated light with the sample is typically frequency dependent. Finally, the phase is directly related to the dynamics of the response of the sample. If  $\tau$  is a typical time scale of such a response (for instance the lifetime of a fluorescent sample, or the mean time-of-flight in a strongly scattering medium) one would consider a modulation frequency such that  $\omega\tau$  is on the order of unity to produce a measurable phase delay. In fluorescence lifetime measurements and for spectroscopy of tissues, typical modulation frequencies are in the range of 1 KHz-100 MHz, but they can be as high as several GHz (1,2). We stress that the frequency  $f$  (or the angular frequency  $\omega$ ) is the frequency of modulation of the light intensity. It should not be confused with the frequency of the light, which is larger by about 6 orders of magnitude. The accurate measurement of the dc, ac, and phase of a signal at a frequency of the order of 100 MHz is not easily accomplished directly. For this reason, the signal is usually down converted to a lower frequency before processing. This stage of the frequency-domain technique is similar to the super heterodyne detection

in AM and FM radios. However, there is here a fundamental difference, which is constituted by the necessity of recovering the phase of the signal with high accuracy. To point out this difference, the down conversion in the frequency-domain is called *cross-correlation*. The main idea of the cross-correlation technique is to mix<sup>†</sup> the detected signal at frequency  $f$ , with a signal at a slightly different frequency  $f+\Delta f$  which is phase-locked to the signal at frequency  $f$  (3). As a result of mixing, one obtains a signal at the beat frequency  $\Delta f$  which contains all the information of phase and amplitude of the original signal at frequency  $f$ . That the output of the mixer still contains the original phase and amplitude information can be demonstrated by multiplying the detected signal  $I_{dc} + I_{ac}\cos(\Phi-\omega t)$  (one of the input of the mixer) by the electronically generated cross-correlation signal  $A + B\cos[\Phi_c - (\omega + \Delta\omega)t]$  (the other input of the mixer):

$$\begin{aligned} & [I_{dc} + I_{ac}\cos(\Phi - \omega t)] \{A + B\cos[\Phi_c - (\omega + \Delta\omega)t]\} = \\ & = AI_{dc} + BI_{dc}\cos[\Phi_c - (\omega + \Delta\omega)t] + AI_{ac}\cos(\Phi - \omega t) + \\ & + \frac{BI_{ac}}{2} \{ \cos[(\Phi_c + \Phi) - (2\omega + \Delta\omega)t] + \cos[(\Phi_c - \Phi) - (\Delta\omega)t] \} \end{aligned} \quad (2)$$

The important frequency components in Eq. (2) are those at zero frequency (the first term on the right hand side of Eq. (2)), which is proportional to  $I_{dc}$ , and at the cross correlation frequency  $\Delta\omega/2\pi$  (the last term on the right hand side of Eq. (2)), whose amplitude is proportional to  $I_{ac}$ , and whose phase is  $\Phi$ , apart from an arbitrary constant phase term. The high frequency components ( $\omega$ ,  $\omega+\Delta\omega$ ,  $2\omega+\Delta\omega$ ) can be filtered out by a low pass filter. The signals at frequency  $f$  and  $f+\Delta f$  must be rigorously phase locked so that  $\Phi_c - \Phi$  is a constant with time. Typical values of  $\Delta f$  range from 10 Hz to 50 KHz.

As a final comment on the basic principles of the frequency-domain, we derive the general relationship between time-domain and frequency-domain quantities. In the time-domain, the response of the sample is characterized by the temporal point spread function (TPSF). The TPSF represents the output signal which corresponds to a  $\delta$  pulse input.

<sup>†</sup> A mixer is an electronic device with two inputs and one output which presents at the output the mathematical equivalent of the product of the signals at the two input ports.

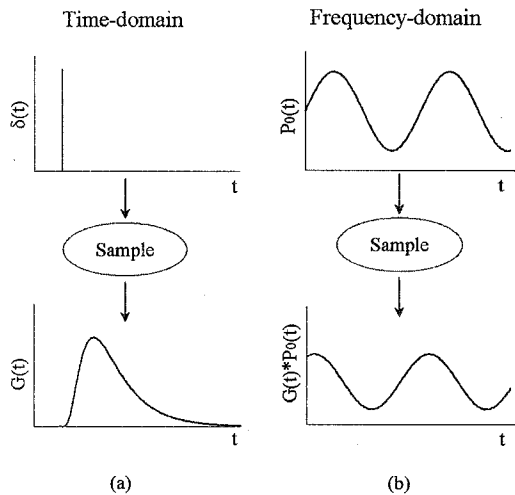


Fig. 1. In a time domain experiment (panel (a)), a short light pulse (ideally a Dirac delta) is used as the optical probe, and one measures the shape of the pulse after interaction with the sample. In the frequency-domain (panel (b)), a periodic signal (of which one harmonic component is illustrated in the figure) is used as the optical probe. After interaction with the sample, the representative harmonic wave is attenuated and is phase shifted with respect to the probing wave. The attenuation (in both the average value or dc, and the amplitude or ac) and the phase shift of the wave are the measured parameters in the frequency-domain. In both figures, the horizontal axis is time, while the meaning of  $G(t)$  and  $P_0(t)$  is explained in the text.

The TPSF is also called the Green's function  $G(t)$ . Figure 1 (a) schematically shows the time-domain response of a sample

In the frequency-domain, the power emitted by the light source can be written in complex notation as  $P_0(t) = P_{dc0} + P_{ac0} \exp[i(\Phi_0 - \omega t)]$ , where the subscripts 0 indicate that the quantities refer to the emission of the source. In the case of linear systems, the response to the oscillating signal  $P_0(t)$  (Fig. 1 (b)) is given by the temporal convolution of  $P_0(t)$  with the Green's function:

$$\begin{aligned}
 G(t) * P_0(t) &= \\
 &= \int_{-\infty}^{+\infty} G(t') P_{dc0} dt' + \int_{-\infty}^{+\infty} G(t') P_{ac0} e^{i[\Phi_0 - \omega(t-t')]} dt' \\
 &= P_{dc0} \int_{-\infty}^{+\infty} G(t') dt' + P_{ac0} \int_{-\infty}^{+\infty} G(t') e^{i\omega t'} dt' e^{i(\Phi_0 - \omega t)} \\
 &= P_{dc0} \tilde{G}(0) + P_{ac0} \tilde{G}(\omega) e^{i(\Phi_0 - \omega t)}, \quad (3)
 \end{aligned}$$

where we have indicated with  $\tilde{G}(\omega)$  the Fourier transform of  $G(t)$ . Eq. (3) shows that the time-domain and the frequency-domain are related by a temporal Fourier transform. The frequency-domain signal is at the same angular frequency  $\omega$  as the source frequency, and its amplitude and phase are given by  $\text{abs}[P_{ac0} \tilde{G}(\omega)]$  and  $\text{arg}[\tilde{G}(\omega)]$ , respectively.<sup>†</sup>

### 3. FREQUENCY-DOMAIN INSTRUMENTATION

#### 3.1. Light Sources and Modulators

In the previous Section, we have shown that frequency-domain spectroscopy requires the modulation of the light source intensity at a relatively high frequency. We have also treated the case of sinusoidal modulation. However, we note that one of the advantages of the cross-correlation technique in conjunction with the fast-Fourier-transform filtering method (which is described in Section 3.3), is the complete insensitivity to harmonic distortion. In fact, the fast-Fourier-transform effectively isolates each harmonic frequency, thus providing rejection of higher harmonics. Not only can this feature be used to correct for the harmonic distortion which is usually present in the intensity modulated signal, but it can be employed for parallel multi-frequency spectroscopy, provided that the light source has a high harmonic content. This latter property is obtained, for instance, by pulsing the light source with a repetition rate equal to the fundamental harmonic frequency (4). It follows that either sinusoidally modulated (at frequency  $f$ ) or pulsed (with repetition time  $1/(nf)$  with  $n$  integer) light sources can be used in frequency-domain spectroscopy. We observe that using pulsed light sources widens the spectral band of the spectrometer at the expense of the duty cycle.

##### 3.1.1. Externally modulated CW. (continuous wave) lasers and arc lamps

The CW emission of lasers or arc lamps can be externally modulated by electro-optical (Pockels cells) (5) or by acousto-optical (3,6) devices. A Pockels cell

<sup>†</sup> Here, "abs" and "arg" indicate the magnitude and the argument, respectively, of a complex number. They are defined as follows:  $\text{abs}(x+iy) = (x^2+y^2)^{1/2}$ ;  $\text{arg}(x+iy) = \tan^{-1}(y/x)$ .

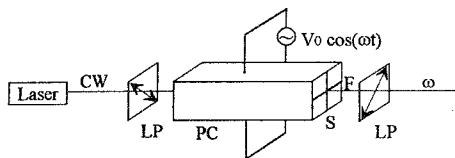


Fig. 2. A Pockels cell used as an optical modulator. The continuous wave (CW) emission of a laser (or an arc lamp after collimation) is sent to a Pockels cell (PC) which is sandwiched between two crossed linear polarizers (LP's). The transmission axes of the LP's make an angle of  $45^\circ$  with respect to the slow (S) and fast (F) axes of the Pockels cell. The alternating voltage  $V_0 \cos(\omega t)$  modulates the refractive index of the Pockels cell along one axis, thus modulating the transmitted light beam intensity at angular frequency  $\omega$ .

is a birefringent crystal which shows a linear dependence of the refractive index along one axis on the strength of an externally applied electric field. By applying a modulated voltage to the Pockels cell, one can vary the relative phase delay of the light polarized along the principal axes of the cell. When such a retardation element is sandwiched between two crossed polarizers, both at an angle of  $45^\circ$  with the principal axes of the cell, it can be used as an intensity modulator. The voltage supplied to the Pockels cell can be either sinusoidal or pulsed. A schematic diagram of an optical modulator based on a Pockels cell is illustrated in Fig. 2.

An acousto-optic modulator is a material which uses the piezoelectric and the photoelastic effects to (a) convert an oscillating electric field into mechanical vibrations, and (b) to achieve spatial variations of the index of refraction, respectively. The amplitude modulation of the oscillating electric field, and therefore of the acoustic wave in the material, results in the modulation of the light intensity transmitted through the material. Alternatively, a standing acoustic wave can be established in the acousto-optic crystal. In this latter case, the intensity modulation can be achieved only at the resonance frequencies of the crystal. Both electro-optical and acousto-optical devices require the light beam to be well collimated. High collimation is provided by lasers, while it requires some optics in the case of arc lamps. Consequently, arc lamps provide a wide-wavelength-band modulated source at the expense of power (typical average powers per unit bandwidth are on the order of  $50 \mu\text{W}/\text{nm}$  after modulation). The

transmission of light modulators strongly depends on the material used. For instance, KDP ( $\text{KH}_2\text{PO}_4$ ) crystals transmit light in the range 230-1200 nm, while lithium-niobate crystals are used between 600 and 4500 nm.

The wavelength of the laser is chosen on the basis of the requirements of the particular application (excitation wavelength of a fluorophore, absorption band of a chromophore, optimal penetration depth in turbid media, etc.). Examples of externally modulated CW lasers used in frequency-domain spectroscopy include argon ion (lines at 275-305, 351, 488, 515 nm), krypton ion (647 nm), He-Ne (633 nm), and He-Cd (325, 354, and 442 nm) lasers. Dye lasers pumped by either argon or krypton lasers afford continuous tunability in a wide spectral range which covers all of the visible band. High pressure xenon arc lamps are usually employed to provide continuous spectral scanning from the UV (230 nm) to the near-infrared (1100 nm), while mercury lamps provide a number of discrete lines. Xe-Hg arc lamps, which contain a mixture of xenon and mercury, show both the broad spectral output of Xe lamps and the line character of Hg lamps; usually, they provide a higher power at the mercury lines. They also provide higher power in the UV than Xe lamps. We note that using an external modulating device imposes some limitations to the modulation bandwidth. Pockels cells provide effective modulations up to about 500 MHz, and acousto-optic modulators up to about 300 MHz. We finally observe that Xe arc lamps can also be directly modulated by supplying them with an oscillating current. However, this approach accomplishes the intensity modulation only at low frequencies, typically below 10 KHz.

### 3.1.2. Pulsed sources

As already discussed, it is possible to achieve a large modulation bandwidth (at the expense of duty cycle) by exploiting the harmonic content of pulsed sources with high repetition rates. These sources can be either mode-locked pulsed lasers (Nd:YAG, Ti:Sapphire, Dye lasers, etc.) (7) or synchrotron radiation (8,9). The repetition rate of the pulses gives the fundamental frequency, whereas the pulse width determines the half width of the power spectrum. The power spectrum of mode-locked lasers extends well above 10 GHz, an upper limit in frequency-domain applications imposed by the optical detectors rather than the light sources. A specific harmonic of the frequency spectrum can be

selected by means of the cross-correlation method discussed in Section 2. The wavelengths of the above mentioned lasers are 1064 nm (532 nm if frequency doubled) for the Nd:YAG, 660-1180 nm (tunable) for the Ti:Sapphire. Depending on the particular dye employed, dye lasers can be tuned in a number of spectral bands: 400-500 nm for coumarin dyes, 560-630 nm for rhodamine 6G, 625-680 nm for DCM, and 675-780 for oxazine 1. A unique pulsed source is provided by synchrotron radiation, which continuously covers all the UV/visible/near-infrared spectrum.

### 3.1.3. Laser diodes and light emitting diodes (LED's)

These light sources can be intensity modulated by driving them with an oscillating current. As a result of the faster response times of laser diodes, they can be modulated at frequencies up to the GHz range. On the contrary, the LED's modulation bandwidth is typically limited to 150 MHz. LED's are incoherent light sources, and they emit light over a wavelength band having a FWHM of about 50 nm. For frequency-domain spectroscopy, one can find LED's in the wavelength region extending from 600 to 1300 nm. As of today, commercially available blue LED's cannot be effectively modulated above 10 MHz, due to their relatively long rise times. Laser diodes emitting in the red and near-infrared can be effectively used in frequency-domain spectroscopy.

### 3.2. Optical Detectors

Optical detectors employed in frequency-domain spectroscopy include photomultiplier tubes (PMT's), avalanche photodiodes (APD), and charge coupled device (CCD) cameras and optical multichannel analyzers (OMA) in conjunction with microchannel plates (MCP's). In all cases, the cross-correlation signal at frequency  $f+\Delta f$  can be mixed with the measured signal at frequency  $f$  in two ways: (1) internally to the detector, by using the cross-correlation signal to modulate the detector gain (see Fig. 3 (a)); (2) externally, by sending the detector output and the cross-correlation signal to the inputs of an electronic mixer (see Fig. 3 (b)). In both cases, the result is the down conversion from the high frequency ( $f$ ) to the cross-correlation frequency ( $\Delta f$ ). The internal mixing procedure has the advantage of avoiding the use of an additional electronic component. Furthermore, the

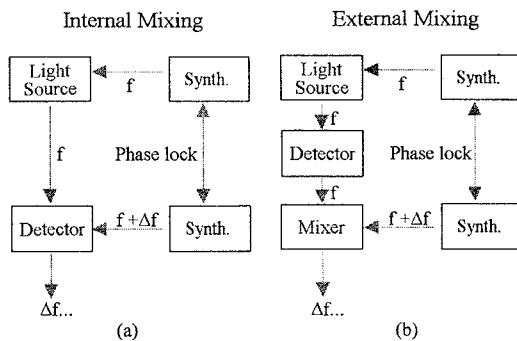


Fig. 3. Internal and external mixing in the frequency-domain. One of the two synthesizers (Synth.) modulates the light source at frequency  $f$ . The second synthesizer provides the signal at frequency  $f+\Delta f$  which modulates the detector gain (panel (a): internal mixing), or which is sent to the second input of an electronic mixer (panel (b): external mixing). In both cases, the two frequency synthesizers are phase locked.

electronic mixer needs to have a 40 dB signal isolation between the ports to avoid leakage of the signal at frequency  $f$  into the output port.

Photomultiplier tubes are extremely sensitive detectors. In fact, the cathode sensitivity is typically 50 mA/W, and a current amplification of about  $10^7$  determines an anode sensitivity as high as 1 A/ $\mu$ W. PMT's can operate in the UV (down to 150 nm), in the visible, and in the near-infrared (up to 1000 nm). In frequency-domain spectroscopy, their gain is modulated by a radio frequency signal which is applied at the second dynode of the amplification chain. Such a signal is about 25 V peak-to-peak on a 50 ohms resistor (i.e. about 32 dBm). The typical rise time of a PMT, which is in the nanosecond range, allows for a modulation bandwidth of several hundred megahertz. A very narrow focusing of the irradiated zone on the photocathode can extend the useful bandwidth up to about 800 MHz. However, careful selection of the electronic components and accurate design of the circuitry are required to avoid radio frequency pickups, especially at frequencies above 200 MHz. The faster response of microchannel plates makes them suitable devices up to several gigahertz. The gain of an MCP is modulated by delivering an oscillating voltage to the cathode. Modulated MCP's in conjunction with OMA's or CCD cameras provide a powerful tool for frequency-domain spectroscopy, microscopy, and

imaging. Avalanche photodiodes can be used when one needs to work at higher modulation frequencies than those allowed by PMT's. The APD output is usually directed to an electronic mixer for down-conversion.

### 3.3. Digital Acquisition and Fast-Fourier-Transform

In Section 2, we have described the cross-correlation technique which down converts the frequency of the detected signal. The major advantage is that we can process a low frequency ( $\Delta f$ ) signal to gather information about the high frequency ( $f$ ) signal. The schematics of the cross-correlation technique is shown in Fig. 3 for both internal and external mixing. In Fig. 4, we illustrate the digital acquisition method, which is described in detail by Feddersen *et al.* (4). The input waveform to the digital processing unit is the result of the mixing of the detected signal with the cross-correlation signal. As already discussed, this waveform contains a harmonic component at frequency  $\Delta f$  which is what we want to filter out and process. The first processing step is the only analog electronics employed. It is a current-to-voltage converter (required by the fact that the PMT output is a current signal) followed by a low-pass amplifier which has a time constant of about  $1/(10\Delta f)$  to attenuate by less than 10% the harmonic frequency  $\Delta f$ . The A/D converter samples the output of the low-pass amplifier at a rate of  $n\Delta f$  where  $n$  is an integer. In this way, the sampling rate is synchronous with the cross-correlation frequency. The sampling theorem (10) states that  $n$  must be at least 2 in order to fully specify the harmonic at  $\Delta f$ . However, a higher sampling rate results in a better discrimination of higher harmonics. Typical values of  $n$  range from 4 to 256. The digital signal processing consists of two steps: (1) synchronously average the data sampled in all of the collected cross-correlation periods; (2) isolate the frequency harmonic at  $\Delta f$  by fast-Fourier transformation. The first filter causes a destructive interference of all the frequencies

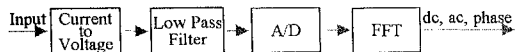


Fig. 4. Digital acquisition scheme. The analog to digital (A/D) conversion is performed after the current-to-voltage stage, and the low pass filter used to reject the radio frequency. The procedure which yields the dc, ac, and phase at a given frequency is performed by a fast Fourier transform (FFT) of the digitized data.

which are not multiple of  $\Delta f$ . The fast-Fourier-transform resolves each one of the harmonics of  $\Delta f$ , and one specific harmonic is retained by discarding all the others. The rejection of higher harmonics is accomplished by more than a factor 2,000 (4). This digital signal processing excels in terms of signal-to-noise. Using this approach, the measurement noise is only determined by the intrinsic limitations due to photon statistics (shot noise) (11).

### 3.4. Analog versus Digital Acquisition

As an alternative to the digital acquisition method described in Section 3.3, analog electronics have been employed in a cross-correlation frequency-domain spectrometer. The analog processing unit is illustrated in Fig. 5. It features a current-to-voltage converter, amplifiers and low-pass filters (integrators). After the current-to-voltage converter, the dc component is obtained by integration with a low-pass filter. A capacitor and a band-pass filter select the ac low frequency component (at the cross-correlation frequency  $\Delta f$ ) which is independently squared and integrated and sent to the computer. Finally, the ac signal at  $\Delta f$  is also sent to a zero-crossing detector for measuring the phase shift of the measured signal with respect to the excitation signal.

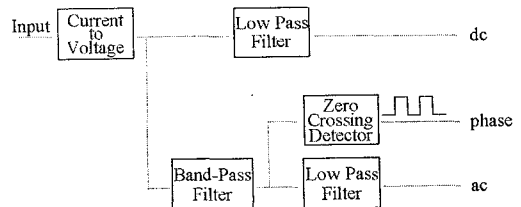


Fig. 5. Analog acquisition scheme. After the current-to-voltage stage, the filtering procedure is performed analogically by a low-pass filter to obtain the dc, and by a band pass filter to isolate the signal at frequency  $\Delta f$ . The ac amplitude of this latter signal is obtained with a low pass filter, whereas the phase is determined by a zero crossing detector.

The above schematics is referred to as the analog processing of frequency-domain data. Even though this scheme is quite simple, it has several disadvantages with respect to the digital method. The first disadvantage is due to the limitation in the bandwidth of the filter employed to isolate the cross-correlation frequency. This filter has to be narrow to reject any

spurious frequencies which result from noise and/or harmonic distortion. Narrow analog filters are difficult to tune and are subject to severe temperature drifts and filter non-linearity. For example, it is common that these filters shift the phase depending on the amplitude of the signal. Also, the center bandwidth cannot be changed without re-tuning or changing the filter. The second disadvantage is related to the zero-crossing detector employed to determine the phase of the signal. A sinusoidal signal directed into a zero-crossing detector is transformed into a square wave, usually a TTL (transistor-transistor logic) level signal. The square wave is produced as the sinusoidal signal crosses a threshold, which is defined as the zero line. In practice, the threshold of a zero-crossing detector oscillates by a few millivolts. The phase of the signal is obtained by taking the difference between the square wave produced by the signal and the square wave produced by a reference. Since the zero-crossing detector uses only one point to measure the phase, it is very sensitive to the signal noise (which causes fluctuations in the triggering time, thus resulting in phase jitter) and to the signal amplitude (the smaller the signal slope with time at the crossing point, the larger the uncertainty in triggering time).

The digital acquisition method and the fast-Fourier-transform data processing appear to be superior to the analog approach in terms of both harmonic rejection, and phase determination. In particular, we observe that the phase measurement in digital systems relies on the digitization of the entire waveform, rather than on one single point as it is done in analog zero crossing detectors.

## 4. APPLICATIONS

### 4.1. Fluorescence Spectroscopy

The fluorescence decay from a fluorophore excited by a  $\delta$  light pulse is described by the exponential law  $\exp(-t/\tau)/\tau$ , where  $\tau$  is the fluorophore lifetime. This means that the Green's function for fluorescence spectroscopy is  $G_{\text{fluor}}(t) = \exp(-t/\tau)/\tau$ , and Eq. (3) yields the following frequency-domain signal:

$$G_{\text{fluor}}(t) * P_0(t) = P_{\text{dc0}} + P_{\text{ac0}} \frac{e^{j \arctan(\omega\tau)}}{\sqrt{1 + \omega^2\tau^2}} e^{i(\Phi_0 - \omega t)}, \quad (4)$$

where the symbols have the same meaning of those in Eq. (3). Equation (4) gives the usual frequency-domain expressions which are valid in the case of a single exponential fluorescent decay:

$$\tau = \omega^{-1} \tan(\Phi - \Phi_0), \quad (5)$$

$$\tau = \omega^{-1} \sqrt{(m_0/m)^2 - 1}, \quad (6)$$

where  $\Phi$  ( $\Phi_0$ ) is the emission (excitation) phase, while  $m$  ( $m_0$ ) is the emission (excitation) modulation. In the presence of a single fluorophore, the two Eqs. (5) and (6) provide independent determinations of the lifetime  $\tau$ . In the case of multiple fluorophores, multi-frequency measurements are required to resolve the different lifetimes (12). The frequency dependence of amplitude and phase for a fluorophore with a lifetime  $\tau$  of 1.5 ns (rhodamine B in water) is shown in Fig. 6 (a). Frequency-domain fluorescence spectroscopy is widely used in biology and biophysics to study the structure and the dynamics of macromolecules (13-16), in cell biology for imaging the intracellular concentration of ions and for the visualization of cellular structures (17), and in analytical and clinical chemistry (18). More recently, fluorescence excitation using two (19) and three (20) photon processes has been demonstrated to sample smaller volumes and to provide higher rejection of excitation light.

### 4.2. Photon Migration

Light propagation in strongly scattering media (tissues) is identified by the expression *photon migration* to underline the usefulness of the particle approach to this problem. In applications like near-infrared tissue spectroscopy, remote sensing of the atmosphere, studies of interstellar dust, etc., light propagation has a diffusive nature and can be modeled by diffusion theory. The Green's function for the diffusion equation with infinite boundary conditions is  $G_{\text{diff}}(t) = \exp[-r^2/(4\nu Dt) - \mu_a \nu t] / (4\pi\nu Dt)^{3/2}$ , where  $r$  is the source-detector separation,  $\nu$  is the speed of light,  $D$  is the diffusion coefficient which is defined as  $1/(3\mu_s')$  with  $\mu_s'$  reduced scattering coefficient, and  $\mu_a$  is the

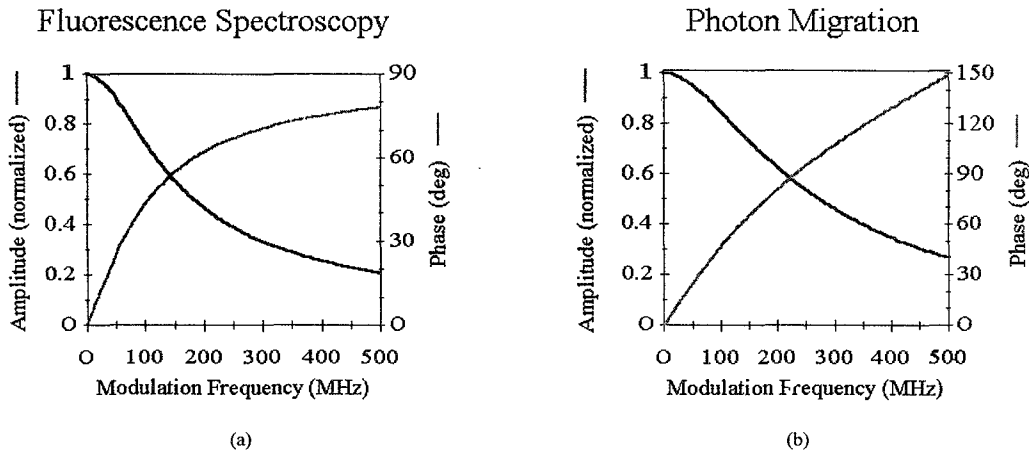


Fig. 6. Frequency dependence of the amplitude and phase of harmonic intensity waves measured by frequency-domain spectroscopy. (a) Fluorescence spectroscopy of a fluorophore with a lifetime of 1.5 ns. (b) Photon migration measurement in an infinite medium having an absorption coefficient of  $0.03 \text{ cm}^{-1}$  and a reduced scattering coefficient of  $10 \text{ cm}^{-1}$ . The source-detector distance is 2 cm. Note that in fluorescence spectroscopy, the phase shift approaches a limiting value of  $90^\circ$  at high modulation frequencies. Such a limiting value does not exist in photon migration measurements.

absorption coefficient. Equation (3) yields the following frequency-domain signal:

$$G_{\text{diff}}(t) * P_0(t) = \frac{1}{4\pi\nu Dr} \left( P_{\text{dc}0} e^{-r\sqrt{\mu_a/D}} + P_{\text{ac}0} e^{-kr} e^{i(\Phi_0 - \omega t)} \right), \quad (7)$$

where  $k = \sqrt{(\nu\mu_a - i\omega) / (\nu D)}$ . Measurements of dc intensity, ac amplitude, and phase of the light transmitted through a turbid medium provide the simultaneous measurement of its absorption and reduced scattering coefficients (21-23). Such a result cannot be accomplished by using the simple intensity information of CW spectroscopy. The frequency-dependence of amplitude and phase for a source-detector separation  $r = 2 \text{ cm}$ , and for a medium with an index of refraction of 1.33 ( $\nu = 2.26 \times 10^{10} \text{ cm/s}$ ),  $\mu_a = 0.03 \text{ cm}^{-1}$ , and  $\mu_s' = 10 \text{ cm}^{-1}$  are shown in Fig. 6 (b). These values are representative of breast tissue at the wavelength of 800 nm (24). Fluorescence signals from tissue-like, strongly scattering media have also been recently investigated in the frequency-domain (25-28).

## 5. CONCLUSIONS

In this Chapter, we have presented the basic principles and the instrumental approaches to frequency-domain spectroscopy. Applications of this technique include fluorescence spectroscopy and photon migration. The frequency-domain capabilities, both basic (high duty cycle resulting in high signal-to-noise and fast acquisition times) and practical (compact and cost effective instrumentation), have recently been exploited to develop several instruments for biomedical applications. For instance, lifetime fluorescence microscopes using the confocal (29), two-photon (30), and pump probe (31) approaches have been used to provide images of cells. In the field of tissue spectroscopy and imaging, frequency-domain prototypes have recently produced a quantitative assessment of hemoglobin saturation in the brain and in skeletal muscle (32,33), as well as the first clinically relevant time-resolved optical mammograms (34). As for future directions, the methods of fluorescence spectroscopy and tissue imaging are likely to be joined in the design of effective clinical tools for sensitive and

specific optical detection of malignant tumors. In this perspective, the frequency-domain technique is certainly among the most promising experimental approaches.

**Acknowledgments.** The Laboratory for Fluorescence Dynamics is supported by the National Institutes of Health (NIH), grant RR03155 and by the University of Illinois at Urbana-Champaign. This research is also supported by NIH grant CA57032 and by a joint Whitaker-NIH grant RR10966.

## 6. REFERENCES

1. J. R. Lakowicz and K. Berndt, "Frequency-Domain Measurements of Photon Migration in Tissues," *Chem. Phys. Lett.* **166**, 246-252 (1990).
2. J. B. Fishkin, S. Fantini, M. J. van de Ven, and E. Gratton, "Gigahertz Photon Density Waves in a Turbid Medium: Theory and Experiments," *Phys. Rev. E* **53**, 2307-2319 (1996).
3. R. D. Spencer and G. Weber, "Measurement of Subnanosecond Fluorescence Lifetimes with a Cross-Correlation Phase Fluorometer," *Ann. N. Y. Acad. Sci.* **158**, 361-376 (1969).
4. B. A. Feddersen, D. W. Piston, and E. Gratton, "Digital Parallel Acquisition in Frequency Domain Fluorometry," *Rev. Sci. Instrum.* **60**, 2929-2936 (1989).
5. E. Gratton and M. Limkeman, "A Continuously Variable Frequency-Domain Cross-Correlation Phase Fluorometer with Picosecond Resolution," *Biophys. J.* **44**, 315-324 (1983).
6. D. W. Piston, G. Marriott, T. Radivoyevich, R. Clegg, T. M. Jovin, and E. Gratton, "Wide-Band Acousto-Optic Light Modulator for Frequency-Domain Fluorometry and Phosphorimetry," *Rev. Sci. Instrum.* **60**, 2596-2600 (1989).
7. J. R. Alcala, E. Gratton, and D. M. Jameson, "A Multifrequency Phase Fluorometer Using the Harmonic Content of a Mode-Locked Laser," *Anal. Instrum.* **14**, 225-250 (1985).
8. E. Gratton, D. M. Jameson, N. Rosato, and G. Weber, "Multifrequency Cross-Correlation Phase Fluorometer Using Synchrotron Radiation," *Rev. Sci. Instrum.* **55**, 486-493 (1984).
9. G. De Stasio, N. Zema, F. Antonangeli, A. Savoia, T. Parasassi, and N. Rosato, "Plastique: A Synchrotron Radiation Beamline for Time Resolved Fluorescence in the Frequency Domain," *Rev. Sci. Instrum.* **62**, 1670-1671 (1991).
10. R. N. Bracewell, *The Fourier Transform and Its Applications*, (McGraw-Hill, Singapore, 1986), pp. 189-194.
11. B. W. Pogue, "Frequency-Domain Optical Spectroscopy and Imaging of Tissue and Tissue-Simulating Media," Ph.D. Thesis (McMaster University, Hamilton, Ontario, Canada, 1995).
12. T. Parasassi, F. Conti, and E. Gratton, "Study of Heterogeneous Emission of Parinaric Acid Isomers Using Multifrequency Phase Fluorometry," *Biochemistry* **23**, 5660-5664 (1984).
13. T. G. Dewey, Ed., *Biophysical and Biochemical Aspects of Fluorescence Spectroscopy*, (Plenum Press, New York, 1991).
14. O. S. Wolfbeis, Ed., *Fluorescence Spectroscopy: New Methods and Applications*, (Springer, Berlin, 1993).
15. J. R. Lakowicz, Ed., *Advances in Fluorescence Sensing Technology II*, *Proc. SPIE* **2388** (1995).
16. J. R. Lakowicz, Ed., *Topics in Fluorescence Spectroscopy: Biochemical Applications*, Vol. 3, (Plenum Press, New York, 1994).
17. R. Nuccitelli, Ed., *Methods in Cell Biology*, (Academic Press, New York, 1994).
18. J. R. Lakowicz, Ed., *Topics in Fluorescence Spectroscopy: Probe Design and Chemical Sensing*, Vol. 4, (Plenum Press, New York, 1994).
19. J. R. Lakowicz and I. Gryczynski, "Tryptophan Fluorescence and Anisotropy Decays of Human Serum Albumin Resulting from One-Photon and Two-Photon Excitation," *Biophys. Chem.* **45**, 1-6 (1993).
20. I. Gryczynski, H. Malak, and J. R. Lakowicz, "Three-Photon Induced Fluorescence of 2,5-diphenyloxazole with a Femtosecond Ti:Sapphire Laser," *Chem. Phys. Lett.* **245**, 30-35 (1995).
21. M. S. Patterson, J. D. Moulton, B. C. Wilson, K. W. Berndt, and J. R. Lakowicz, "Frequency-Domain Reflectance for the Determination of the Scattering and Absorption Properties of Tissue," *Appl. Opt.* **30**, 4474-4476 (1991).
22. B. J. Tromberg, L. O. Svaasand, T. T. Tsay, and R. C. Haskell, "Properties of Photon Density Waves in Multiple-Scattering Media," *Appl. Opt.* **32**, 607-616 (1993).

23. S. Fantini, M. A. Franceschini, J. B. Fishkin, B. Barbieri, and E. Gratton, "Quantitative Determination of the Absorption Spectra of Chromophores in Strongly Scattering Media: a Light-Emitting-Diode Based Technique," *Appl. Opt.* **33**, 5204-5213 (1994).
24. G. Mitic, J. Kölzer, J. Otto, E. Plies, G. Sölkner, and W. Zinth, "Time-Gated Transillumination of Biological Tissues and Tissue-like Phantoms," *Appl. Opt.* **33**, 6699-6710 (1994).
25. M. S. Patterson and B. Pogue, "Mathematical Model for Time-Resolved and Frequency-Domain Fluorescence Spectroscopy in Biological Tissue," *Appl. Opt.* **33**, 1963-1974 (1994).
26. C. L. Hutchinson, T. L. Troy, and E. M. Sevick-Muraca, "Fluorescence-Lifetime Determination in Tissues or Other Scattering Media from Measurement of Excitation and Emission Kinetics," *Appl. Opt.* **35**, 2325-2332 (1996).
27. X. D. Li, M. A. O'Leary, D. A. Boas, B. Chance, A. G. Yodh, "Fluorescent Diffuse Photon Density Waves in Homogeneous and Heterogeneous Turbid Media: Analytic Solutions and Applications," *Appl. Opt.* **35**, 3746-3758 (1996).
28. A. E. Cerussi, J. S. Maier, S. Fantini, M. A. Franceschini, W. W. Mantulin, and E. Gratton, "Experimental Verification of a Theory for the Time-Resolved Fluorescence Spectroscopy of Thick Tissue," *Appl. Opt.*, *in press*.
29. J. A. Dix and A. S. Verkman, "Pyrene Eximer Mapping in Cultured Fibroblasts by Ratio Imaging and Time-Resolved Spectroscopy," *Biochemistry* **29**, 1949-1953 (1990).
30. D. W. Piston, D. R. Sandison, and W. W. Webb, "Time-Resolved Fluorescence Imaging and Background Rejection by Two-Photon Excitation in Laser Scanning Microscopy," *Proc. SPIE* **1640**, 379-389 (1992).
31. C. Y. Dong, P. T. C. So, T. French, and E. Gratton, "Fluorescence Lifetime Imaging by Asynchronous Pump-Probe Microscopy," *Biophys. J.* **69**, 2234-2242 (1995).
32. R. A. De Blasi, S. Fantini, M. A. Franceschini, M. Ferrari, and E. Gratton, "Cerebral and Muscle Oxygen Saturation Measurement by Frequency-Domain Near Infra-red Spectrometer," *Med. Biol. Eng. Comput.* **33**, 228-230 (1995).
33. W. J. Levy, S. Levin, and B. Chance, "Near-Infrared Measurement of Cerebral Oxygenation," *Anesthesiology*. **83**, 738-746 (1995).
34. H. Jess, H. Erdl, K. T. Moesta, S. Fantini, M. A. Franceschini, E. Gratton, and M. Kaschke, "Intensity-Modulated Breast Imaging: Technology and Clinical Pilot Study Results," *OSA Trends in Optics and Photonics on Advances in Optical Imaging and Photon Migration*, R. R. Alfano and J. G. Fujimoto, eds. (Optical Society of America, Washington, DC 1996), Vol. 2, pp. 126-129.